

**The Effect of Clay Swelling on Fracture Flow in the  
Paintbrush Nonwelded Unit of the Topopah Spring Tuff**

**Timothy J. Kneafsey, Curt Oldenburg, and Rohit Salve**

**Abstract**

To evaluate flow processes such as matrix swelling and particle redistribution that might explain the decline in water uptake in a subvertical fracture system with time in field experiments, we performed a laboratory experiment using a 12 cm diameter x 21.6 cm long core with an axial saw-cut fracture. The core was extracted from the argillic Tpbt2C layer of the Paintbrush nonwelded tuff (PTn) at Yucca Mountain, Nevada. Flow through the PTn is thought to be primarily through the highly porous matrix. Large fractures and faults in the PTn may also provide pathways for flow through the unit; thus we need to better understand flow through these faults.

Permeability, inlet and outlet flow rate and the volume change of the rock core (contained in a pressure vessel) were monitored while flow occurred through the fracture and matrix. Water containing various sodium chloride concentrations (1 M to 0 M) was flowed through the fracture to observe the effect of salt concentration on fracture permeability in the smectite-rich rock core. The permeability of the fracture declined with declining salt concentration and

increased with increasing salt concentration. The sample swelled initially, despite the high salt concentration (1 M) of the inlet water.

## **1. Introduction**

The Paintbrush nonwelded unit (PTn) of the Topopah Spring Tuff has properties substantially different from the fractured rhyolitic welded tuff units at Yucca Mountain, Nevada (Moyer et al., 1996). This unit lies approximately 140 to 270 meters (SE to NW) above the potential high-level nuclear waste repository and varies in thickness from about 180 to 20 meters (north to south) across the potential repository footprint. The depth of the top of the layer ranges from ground surface to over 120 m below ground surface (Moyer et al., 1996). Water flowing through the fractured welded tuff units at Yucca Mountain flows primarily in the fractures. The PTn is less fractured, more porous, and much softer (less indurated) than the welded units. Flow through this unit is thought to occur primarily through the matrix, as well as through major fractures and faults (Bodvarsson et al., 1999).

Flow through the PTn will substantially affect the performance of the potential high-level radioactive waste repository being evaluated for the site. It is thought that the PTn dampens flow pulses from the ground surface to the repository horizon and causes substantial lateral flow, providing an umbrella for the repository (Bodvarsson et al., 1999). Faults and fractures through the unit may

disrupt this lateral flow diversion, and thus flow through these features must be better understood.

To gain a better understanding of flow through the PTn, field experiments were conducted in a side alcove (Alcove 4) of the Exploratory Studies Facility (ESF) at Yucca Mountain. The ESF is an 8 km long tunnel beneath Yucca Mountain designed to provide access for scientific investigation of flow processes that occur under ambient and thermally perturbed conditions. In the field experiments, water from well J-13 containing tracers (20 ppm LiBr, and at different times KF at 1g/l, 2,4-difluorobenzoic acid at 0.017 g/l, and 2,3,6-trifluorobenzoic acid at 0.017 g/l) was introduced at constant head into a 0.3 m section of a borehole that intersected a fault. About three meters below the injection borehole, a slot had been mined to collect water reaching that location. The water intake rate was continuously recorded and the slot monitored for seepage (Salve and Oldenburg, in press). Boreholes adjacent to the injection borehole were monitored for changes in saturation and water potential before, during, and after the controlled release of water. A total of 193 liters of water was released under constant-head conditions during seven distinct releases over two weeks, between October 21 and November 5, 1998. Between November 30 and December 2, 1999, an additional 136 liters of water were introduced into the same interval during three distinct events. Each release event lasted 4–7 hours, during which time 17–56 liters of water entered the injection zone. Intake rates

decreased as more water was introduced into the fault, from an initial rate of  $\sim 150 \text{ ml min}^{-1}$  to  $\sim 50 \text{ ml min}^{-1}$  after 193 liters of water were released (Salve and Oldenburg, in press). No water was collected in the slot; however, water was seen at the slot on the last day of testing. The matrix adjacent to the fault apparently imbibed water more than 1 m from the water-release point.

The field experiments provided valuable insights into flow processes in the PTn. However, they also raised important questions about the mechanisms controlling flow in fractures and the matrix in this unit. Several hypotheses were postulated to explain the reduction in intake of water into the system:

- 1) Decreasing head gradient - the head gradient from inlet to extent of flow decreases as extent increases (i.e., the head at the inlet and outlet remain constant, but the distance between them increases reducing the gradient), (Figure 1a fracture, Figure 1b matrix),
- 2) Air trapped in the fracture blocked water flow as was observed in soils by Faybishenko (1995).
- 3) Fracture permeability is reduced because of clay swelling and redistribution of fines (Figure 1c).

A decreasing head-gradient over the duration of the experiment would be expected in situations where the flow is capillary driven (rather than gravity driven). This type of flow occurs in horizontal and narrow vertical fractures.

The decline in the matrix's ability to absorb water was not investigated here, although we did collect data on water uptake during the initial injection. Additional work is needed to better address the sorptivity of the rock. We believe the effects of fracture blockage due to air and subsequent air dissolution would provide an eventual increase in flow, thus we did not further consider this. Clay swelling has been observed to reduce fracture permeability in laboratory experiments using a clay layer on rigid fracture walls (Carter, 1986). Here, laboratory experiments were performed to evaluate the impact of clay swelling and particle redistribution on permeability through PTn fractures. In these experiments, described in detail below, water with varying salt concentration was flowed through a saw-cut fracture in a smectite-rich rock core extracted from the Tpbt2C layer at Yucca Mountain. The varying salt concentration was applied to influence clay swelling, with high salt concentration expected to reduce swelling and lower concentrations allowing swelling (Norrish, 1955). The volume of the rock and the permeability were measured over time.

## **2. Samples**

Three samples were obtained from the PTn from Alcove 4. These samples were cored from the alcove wall using a 5-inch outer diameter x 10-inch core drill. Two of the samples were taken from a fault, and a third was taken from a lower layer away from the fault (See Figure 2). The two samples from the fault

(SPC00562013, SPC00562014) were received in pieces too small for laboratory flow investigations. In the laboratory investigation, we used the intact core sample (SPC00562012) from below the argillic layer. The core was pinkish-tan, contained visible layers, and had sporadic hard grains within the soft matrix. The core was 12 cm in diameter and 22.8 to 24 cm long (Figure 3). Mineral content was determined using x-ray diffraction (XRD) analysis from scrapings taken from both ends of the core.

Table 1. XRD Analyses Indicating Approximate Weight Percent

Sample	Opal-CT	Quartz	Plagioclase	K-Feldspar	Magnetite	Clinoptilolite	Illite +10A Mica	Smectite	Amorphous and Below Detection
SPC00562012	-	1	7	7	1?	3	3	76	-

The core contains about 76% smectite, which is a swelling clay. The smectite content is towards the upper end for this mineral in this unit, but it is not uncharacteristically high (Moyer et al., 1996). The presence of smectite in such abundance indicates a high degree of mineral alteration from the original mineral assemblage.

### 3. Flow Experiment

A detailed schematic of the experimental setup is presented in Figure 4. The sample was ground flat on the ends and cut axially into two halves. To avoid wetting the sample, air cooling was used during grinding and cutting. Six

Mylar® shims (190 micron x ~0.6cm x ~5 cm) were placed between the two halves, with the long direction parallel to the axis of the core (in the flow direction) approximately 3 cm from the edges. The core was reassembled with the shims and placed inside a rubber sleeve having a slightly higher internal diameter (12.1 cm) than the core outer diameter. Aluminum endcaps (12.1 cm o.d. x 2.54 cm), with a pattern milled into the inner end to allow distribution of the water over the entire core end, were inserted into the sleeve adjacent to the core. The milled pattern was connected to two fittings on each endcap to allow for flow into or out of the core. Two Viton® bands 8.9 cm diameter x 1 cm wide were stretched and placed around the rubber sleeve over each endcap to minimize leakage. To further minimize leakage into the core, we wrapped a nylon cord twice around the rubber sleeve over the endcap between the two Viton® bands, and secured the cord with an elastic strap. Two sets of elastic straps were also placed axially to hold the endcaps to the core.

The core assembly with rubber sleeve and end caps was placed into a large pressure vessel and suspended by two stainless steel tubes connected to the top endcap and the pressure vessel top. Two Teflon® lines were connected from the bottom end cap to the flow-throughs on the bottom of the pressure vessel. The pressure vessel was pressurized using an Isco Series D syringe pump (SN 621240038-95061, 500 ml capacity), with water as the confining fluid. The confining water was dyed with FD&C Yellow #6 dye to allow easy identification

of leakage, both to the outside of the vessel (external leak) and into the rock core (internal leak). The pump was used in the constant pressure mode, and the volume indicator on the pump controller was used to determine changes in the confining-system volume. These changes include leakage and swelling/shrinkage of the core.

Water was introduced into the core using a Mariotte bottle to establish a constant head. The Mariotte bottle was placed on an analytical balance to monitor the mass of water introduced. Water passing through the core was collected in a vessel on another analytical balance. Both balances were connected to computer-based data acquisition systems. The syringe pump pressure was maintained automatically by the Isco pump, and the pump volume was recorded manually.

#### **4. Measurements**

To evaluate clay swelling and imbibition into the rock, we used the following scheme once confining pressure was applied to the sample:

1. Measure sample (fracture) gas permeability.
2. Introduce high-ionic-strength water (to establish the nonswelling case) until steady-state flow occurs.
3. Purge water from fracture and measure gas permeability.
4. Introduce medium-ionic-strength water until steady-state flow occurs.



5. Purge water from fracture and measure gas permeability.
6. Introduce fresh water until steady-state flow occurs.
7. Purge water from fracture and measure gas permeability.
8. Introduce high-ionic-strength water until steady-state flow occurs.
9. Purge water from fracture and measure gas permeability.

One molar NaCl was used as the high-ionic strength water, 0.5 M NaCl was selected as the medium ionic strength water, and distilled deionized water was used as the fresh water. Experimental results of Carter et al. (1986) indicated that 0.75 M NaCl was sufficient to reduce clay swelling in artificial fractures containing a coating of swelling montmorillonite clay. Carter et al. (1986) also reported that lower salt concentrations resulted in swelling and reduced the flow through the laboratory fractures. Norrish (1955) showed data indicating that swelling is limited near 1 M NaCl.

Gas permeability measurements were conducted by draining the fracture and flushing nitrogen gas through until no water was produced. Individual measurements of gas pressure at the inlet and outlet, and gas flow rate were recorded at as many as 25 flow rates. Permeability was calculated from the entire data set collected over the range of inlet pressures (typically not exceeding 2 psig) using the following relation (Scheidegger, 1974):

$$k=(2q_o\mu p_o L)/(p_L^2-p_o^2) \quad (1)$$

where  $k$  is permeability ( $L^2$ ),  $\mu$  is the viscosity ( $ML^{-1}T^{-1}$ ),  $p_o$  ( $ML^{-1}T^{-2}$ ) is the pressure at location “o” (outlet),  $p_L$  is the location at location “L” (inlet).  $q_o$  ( $LT^{-1}$ ) is the gas velocity ( $LT^{-1}$ ) at location “o,” calculated by dividing the measured flow rate by the area for flow determined by iteration . The slope of the plot of  $q_o$  versus  $(p_L^2-p_o^2)$  is equal to  $k/(2\mu L p_o)$ , allowing calculation of  $k$  with the known viscosity, distance, and outlet pressure. Flow rate versus inlet and outlet pressures without the core present were also measured to allow for correction of the system flow resistance in the measurements. The correction was made using Equation 1 assuming that the system (including all tubing and flow-throughs) and core were in series. Using appropriate areas ( $A$ ) and measured flow rates ( $Q_o$ ), Equation 1 becomes

$$Q_o p_o = \frac{kA}{2\mu L} (p_L^2 - p_o^2) \quad (2)$$

The term  $(kA/2\mu L)$  was obtained for both the system and the core, and the core permeability was determined.

During the flow experiments, the water introduction rate, water collection rate, vessel pressure, room and vessel temperature, confining pump volume, and

confining pump flow rate were recorded. The water introduction and collection rates provide us with flow rate through and imbibition into the rock core. The vessel pressure was monitored at the syringe pump, using the pump pressure transducer. This was intermittently rezeroed by isolating the pump from the vessel and opening it to the atmosphere. During the experiment, the maximum drift of the zero point was 3 psi (100 psi confining pressure); however, a check following the experiment indicated a drift of 7 psi. The syringe pump volume and pump flow rate provide indications of volume change and rate of volume change within the system, as well as leakage.

Before the experiment, the vessel and lines were pressure-tested. Several leakage points were identified. Minor leaks were detected in line connections from the pump to the pressure vessel and in connections at the pump. These were easy to find and the connections were tightened. At the start of the experiment, a recalcitrant leak was persisted at the end of the vent line despite efforts to tighten the plug. This leak was plugged at an early stage in the experiment. Leakage was also observed into the rubber sleeve containing the sample (or the aluminum cylinder blank). On system disassembly, dye stains on the end caps indicated that leaks also occurred between the rubber sleeve and the end cap. The extent of these leaks will be addressed below. Leakage is an interference to measuring the swelling of the core, and only a portion of the total leakage rate can be quantified.

## 5. Results

### 5.1 Flow

The cumulative water introduced and collected and flow rates are shown in Figure 5a for 0–45 hours and 5b for 0–377 hours. (The time axis only shows time when water was introduced to the system. In reality, a 2-day break occurred after 7.75 hours, a 17-hour break occurred after 15.6 hours, a 17 hour break occurred after 22.4 hours, a 3 hour break after 45.9 hours, and a 12 hour break after 305 hours.) Constant flow was not established in the early phase of the experiment. The initial start and restarts following breaks were associated with highly variable inlet and outlet flow rates, but with the exception of the initial water introduction, steady state (water inflow and outflow rates approximately the same) was achieved within a few hours of startup.

Water with 1 M NaCl was flowed until a steady state was reached between inlet and outlet flow rates, which took a total of about 16 hours. During the initial introduction of water (Figure 5a), no water was produced at the outlet. After the introduction of about 750 ml of 1 M NaCl, water began to flow out of the fracture. The steady flow rate established during the initial 1 M NaCl flow was above 0.5 ml/min. Clay swelling was not expected during this flow phase; thus this would be the baseline flow rate. Following the 1 M NaCl, 0.5 M NaCl was introduced for a total of about 30 hours. The system rapidly reached steady state

with respect to flow rate because the rock was already satiated with water. After the system attained steady state, fresh water (0.0 M NaCl) was introduced (Figure 5b). Within a few hours, both the rate of introduction and collection began to decline and continued to decline over 260 hours to less than one-third of the baseline value. The final water introduced was 1 M NaCl. Water introduction and collection rates increased immediately to above the final rates observed with the 0.0 M NaCl and then declined slightly over the 72 hours of flow.

## 5.2 Permeability

Gas permeability values (measured with nitrogen) and the corresponding calculated apertures (flat parallel plate assumption,  $aperture = \sqrt{12k}$ ) for the core are shown in Table 2. Permeability was measured before introduction of any water, once following 8 hours of 1 M NaCl introduction, again after an additional 6 hours of 1 M NaCl introduction, after 7 hours of 0.5 M NaCl introduction, after another 24.5 hours of 0.5 M NaCl, after 260 hours of 0.0 M NaCl, and finally after 72 hours of 1 M NaCl introduction. The permeability of the fracture decreased from the initial dry state with the introduction of the 1 M NaCl, and then at each subsequent measurement except for the last one, when the 1 M NaCl was reintroduced.

Table 2. Core Permeability

Measurement	Following	Fracture Permeability (m <sup>2</sup> )	Calculated Fracture Aperture (microns)
1	Initial	1.61x10 <sup>-09</sup>	139.1
2	8 hours 1 M	4.02x10 <sup>-10</sup>	69.4
3	14.3 hours 1M	2.63x10 <sup>-10</sup>	56.2
4	7 hours of 0.5M	1.81x10 <sup>-10</sup>	46.7
5	31.5 hours of 0.5M	1.76x10 <sup>-10</sup>	46.0
6	260 hours 0.0M	9.91x10 <sup>-11</sup>	34.5
7	72 hours 1.0M	1.17x10 <sup>-10</sup>	37.4

### 5.3 Swelling

Swelling was monitored using the volume of confining water in the syringe pump. This volume is plotted in Figure 6a. A positive change in volume here indicates swelling of the core. Immediately upon introduction of the 1 M NaCl, the core began to swell. The swelling on the first day amounted to about 0.5% of the core volume. If we assume that the leakage rate just prior to the introduction of water is constant throughout the experiment, an adjusted swelling volume can be calculated. These data are plotted in Figure 6b. Total swelling indicated (considering this assumption) is roughly 4% of the core volume. The constant leak rate assumption was partially justified by the final adjusted slope (following the introduction of all water) being relatively flat. The actual leakage rate probably declined over the duration of the experiment as small leaks became plugged. It is reasonable to expect the actual swelling is somewhere between the initial 16 ml (Figure 6a) and the corrected 100 ml.

#### 5.4 Ionic strength

The electrical conductivity of the collected water was measured and compared to inlet water samples of known concentration (Figure 7). The data are reported as molarity NaCl, although ion exchange may have occurred, changing the chemistry of the effluent. At no point did the effluent ever contain 1 M NaCl.

The first water collected had an electrical conductivity indicating a NaCl molarity below 0.9. As expected, upon introduction of the 0.5 M NaCl, the NaCl concentration in the collected water declined. The decline continued upon introduction of the 0.0 M NaCl, with tailing occurring. Upon introduction of the final 1 M NaCl, the NaCl concentration in the collected water climbed to 0.37 at the end of the test.

#### 5.5 Observations of Effluent and Solids Produced

Solids and dyes were washed out of the core during the experiment. Orange dye (FD&C Yellow # 6) from the confining water and blue dye (introduced to the fracture and over one end of the core during a pressure vessel pressurization mishap) were present in the effluent. A description of the collected water and solids is provided in Table 3. The blue color is believed to be eluted dye and dyed clay particles (Figure 8) as settling occurred in many cases.

Table 3. Description of Effluent Water and Solids.

Condition	Effluent Description over Time
Initial 1 M NaCl	Light orange, with several large (~100 microns) blue particles
0.5 M NaCl	Decreasing orange color intensity with time, some light color flocc-like particles and some orange-blue flocc-like particles
0.0 M NaCl	Orange and orange-blue flocc-like particles decreasing in number, several clear samples collected, then fine blue particles produced. At lowest salt concentration the blue color did not settle over several weeks.
Final 1 M NaCl	Suspended blue to settled blue, to clear.

## 6. Discussion

Clay swelling was expected to occur at salt concentrations below 0.75 M NaCl (Carter, 1986). Therefore, we expected to see no influence initially on the fracture permeability with 1 M NaCl, but we did expect reductions in permeability (from swelling and particle redistribution) with salt concentrations below 0.75 M.

Upon the final introduction of 1 M NaCl, we expected to see an increase in permeability. With the exception of the permeability decrease and swelling occurring with the initial 1 M NaCl introduction, the permeability behavior of the system was as expected. The applied stress within the pressure vessel (100 psi) was below lithostatic (~500 psi) thus, the effects observed may not have been of the magnitude observed in the field because the higher stress would tend to press the swelling fracture together.

Prediction of the magnitudes of the permeability changes was not performed. If swelling occurred and the core halves remained rigid and separated by the constant-size shims, the geometry of the aperture would not change, and no



influence of salt concentration on permeability would be observed. The core halves did not behave rigidly, however. The difference between the shim thickness (190 microns) and the initial calculated aperture (140 microns) probably results primarily from the shims being pressed into the rock upon pressurization. The stress was concentrated at the location of the shims. From geometrical considerations, the magnitude of the stress at the shims was about 13.5 times the applied stress. Upon experiment completion and fracture opening, we found that the shims had been pressed into the matrix slightly, or the surrounding matrix had swelled about them, reducing the aperture size. From these observations, it was not possible to determine whether swelling occurred under the shims, although swelling would be expected.

Both the permeability measurements and flow quantification are roughly consistent with each other. Gas permeability and liquid flow rate declined with decreasing salt concentration, indicating that the fracture aperture closed as the rock swelled. The two different phases (gas and water) used to measure the permeability interact differently with the system. When the sample is saturated with water, gas permeability measurements will capture only the fracture permeability, because the capillary-held water will preclude gas flow in the rock matrix. Residual fracture water saturation will impact the measurements by reducing the measured permeability. Because of the high correlation coefficients of the gas permeability measurements for the range of induced flow rates, we

believe that there was no free liquid water in the fracture during the measurements. Water was generally cleared from the system by many hours of drainage, followed by forcing gas through the system.

Water, on the other hand, interacts with both fractures and the water-satiated matrix. Water may flow through the matrix, and if the matrix permeability is high enough, matrix flow may dominate. The matrix permeability of the PTn in this region is about  $1.6 \times 10^{-16} \text{ m}^2$  (Moyer et al., 1996) which is 5-6 orders of magnitude lower than the fracture permeability. For the core geometry, this corresponds to a matrix flow of only about 0.5 percent of the fracture flow if the aperture is 30 microns.

The initial swelling when the 1 M NaCl was introduced was not expected. A possible explanation for this swelling is that water was present in the rock prior to the introduction of the 1 M NaCl. The core was air dried before installation into the pressure vessel. However, in an earlier attempt to pressurize the vessel with the core inside prior to the startup of the experiment, the rubber sleeve-endcap system failed, resulting in the wetting of the core (but not saturation or saturation) with blue-dyed water. The core was wetted over 80% of the fracture faces and on one end. Only a small amount of water (estimated to be on the order of 100 ml) was forced into the core. The core was air-dried again for 8 days prior to reassembly. Water remaining in the rock could have diluted the

imbibing 1 M water resulting in an overall concentration in the rock within the range where swelling might be expected. This is consistent with the electrical conductivity data. The total volume of fresh water needed to reduce the 1 M influent NaCl concentration to below 0.75 M in the sample would be 250 ml. The rock porosity is approximately 50% (Moyer et al. 1996); thus, 250 ml of water corresponds to an initial water saturation of approximately 20%. It is possible that the initial saturation (called “air-dry”) was that high. The 0.5% volume increase upon the initial 1.0 M NaCl introduction was very high considering the applied pressure and salt concentration.

Following the initial swelling with the 1 M NaCl solution, additional swelling occurred with the 0.5 M NaCl. Greater swelling occurred with the introduction of the fresh water. This swelling continued throughout the fresh water flow. The rate of swelling was reduced by the introduction of the final 1 M NaCl water. Continued swelling was indicated by the syringe pump following the completion of all water flow. This continued swelling indicates either that the assumed leakage rate was incorrect, or that swelling occurred as the water and salt within the core became redistributed, or that another effect such as temperature altered the system. Temperature would affect the expansion and contraction of the pressure vessel, confining water, tubing, and syringe pump, with each of these changes indicating an apparent swelling or shrinkage. Increases in temperature

should be associated with apparent swelling. Temperature and pump volume are shown in Figures 9a and 9b.

## **7. Leaks**

The bleed valve on the top exterior of the vessel provided a leak smaller than one milliliter per hour. This leak was sealed early in the flow experiment, as indicated by the absence of collectable orange dye. No other leaks were detected on the outside of the vessel, but other leaks were later identified on the inside of the vessel. Pressure testing of the vessel and tubing had been performed prior to placing the rock core into the vessel, with no indicated leakage. An aluminum blank was used in the second phase of the pressure testing in place of the rock core, and some leakage was noted between the rubber sleeve and the end caps. The amount of leakage was not quantified. Upon removal of the rubber sleeve (at the end of the experiment in which the rock core was in place), orange dye stains were present on the inside of the rubber sleeve at the location of the end caps, indicated that some leakage occurred there. The color intensity of the dye stain decreased rapidly over the length of the end cap, with very little being present near the core.

Depending on the size of the leak(s), leakage from the vessel reduces the ability to accurately determine the volumetric change of the sample. A leak rate large in comparison to the swelling of the sample could completely overshadow the

measurement of swelling. The total leak rate was less than 0.2 ml/hr, and this rate was observed both before and after the experiment. Leakage of the dyed confining water (tap water ~ fresh) into the rubber sleeve may introduce water at a different salinity than the intentionally introduced water. An attempt to quantify the leak was made. Samples of the collected water were analyzed for Yellow Dye #6 using a spectrophotometer and a sample of the confining water as the standard. This quantification indicated approximately 8 ml of water leaked into the system in the first 165 hours of flow (During this period, 3411 ml water was introduced and 2615 ml collected.) This small leak was trivial compared to the volume of water intentionally introduced, and consequently we do not believe that the leaked water had a significant impact on the swelling of the sample.

Comparing Figures 6 and 7, we find that most of the introduced salt has been removed by late in the 0.0 M flow, and continued swelling is indicated. Figure 7 shows the NaCl concentration of the water being introduced and leaving the core, as well as the mass of NaCl introduced and collected. Note that while the initial 1 M NaCl solution was introduced, the maximum concentration collected was 0.87 M. It is possible that separation between clay layers upon interaction with the 1 M NaCl decreased in response to the highly saline water, thus expelling more fresh water between the layers and diluting the effluent.

Early in the experiment, the disparity between the introduced and collected salt mass grew rapidly as the NaCl accumulated in the core. On introduction of the fresh water, almost all of the NaCl was recovered. This was not expected, because diffusion was the mechanism expected to return the salt to the fracture flow. If we assume that the initial 1 M water wetted the core from the aperture outward in a piston-type flow, all the 1 M water would be held within about 5 cm of the aperture. The diffusive time constant for the system ( $\tau=2L^2/D$ ,  $D=1.24\text{e-}9 \text{ m}^2/\text{s}$ ,  $L = 0.049 \text{ m}$ ) is about 45 days, indicating that diffusion alone is not responsible for the removal of the NaCl over the 260 hours of fresh water flow. If a significant amount of water was present in the core at the start of the experiment, this water would have been pushed ahead of the salt front towards the rubber sleeve reducing the diffusion distance to the fracture in the cylindrical core. Swelling and shrinking processes may also serve to advect fluid into or out of the rock.

The observation that effluent water contained particles confirms that particle redistribution occurs. At very dilute salt concentrations, the clays would tend to delaminate, resulting in suspensions that would be difficult to settle. This did occur. At higher salt concentrations, clays would tend to flocculate, and at higher salt concentrations, we saw larger particles and more rapidly settling suspensions. The fresh flows resulting in slow settling suspensions would tend to erode fractures in the PTn, increasing permeability. The opposite occurred,

indicating that swelling of the rock was the dominant permeability control mechanism.

## **8. Conclusions**

Clay swelling in the PTn reduced the permeability in our saw-cut fracture. With the exception of the initial swelling occurring with 1 M NaCl, the trend of swelling and reduction in permeability was predictable, with increased swelling resulting in reduced fracture permeability occurring at lower salt concentrations.

Particle redistribution was also observed, but was of a lesser magnitude over the duration and conditions of the experiment. Particle redistribution was indicated by particles observed in the effluent, with those resulting from lower salinity flows not settling well and those from higher salinity flows settling more easily and being larger and more compact. If particle redistribution were controlling the flow, the permeability should have increased because of particle erosion once low salinity water was introduced. The suspended particles at low salt concentrations were difficult to settle and would not deposit easily (reducing permeability). These particles would likely move at Yucca Mountain.

Imbibition-controlled flow was also observed in the beginning of the experiment. Flow into the core was observed, with the flow rate declining until satiation, but

no outflow was observed until the core was satiated. Once satiation occurred, further accumulation in the core was not observed.

In the field experiments, it was not possible to collect outflow. All of the above mechanisms probably contributed to that. In the laboratory experiment, swelling occurred during the initial water introduction (when imbibition-controlled flow would have occurred) and a decrease in the fracture permeability was measured. Continued decreases in fracture permeability occurred with decreasing salt concentrations, indicating that swelling was the major cause of the permeability reduction. In field tests at Yucca Mountain, the initial wetting of the drying rock probably induced swelling. This swelling would have decreased permeability reducing the ability of the system to uptake water at the initial rates.

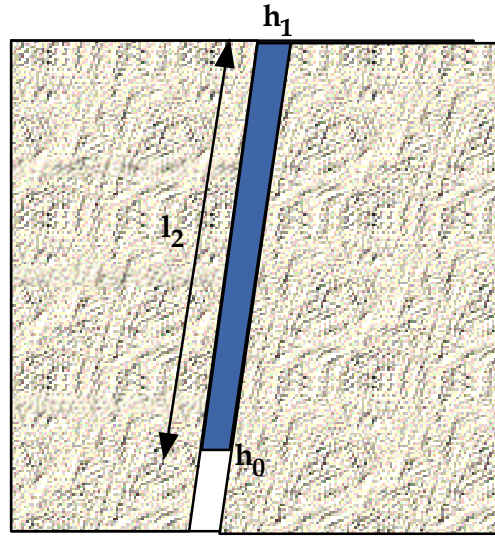
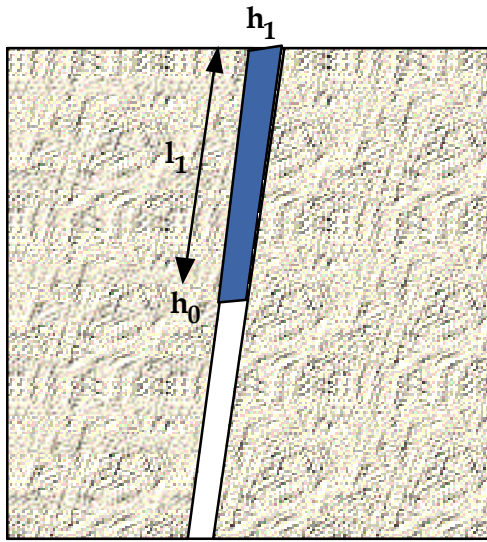
## **9. Acknowledgements**

This work was supported by the Director, Office of Civilian Radioactive Waste Management, U.S. Department of Energy, through Memorandum Purchase Order EA9013MC5X between Bechtel SAIC Company, LLC and the Ernest Orlando Lawrence Berkeley National Laboratory (Berkeley Lab). The support is provided to Berkeley Lab through the U.S. Department of Energy Contract No. DE-AC03-76SF00098. Technical reviews by Jil Geller and Yongkoo Seol and the editorial review by Dan Hawkes were greatly appreciated.

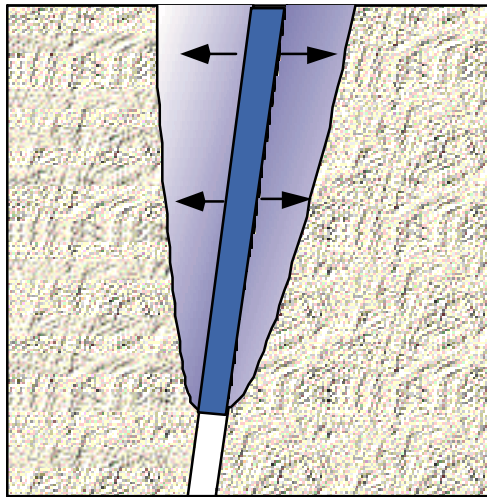


## References

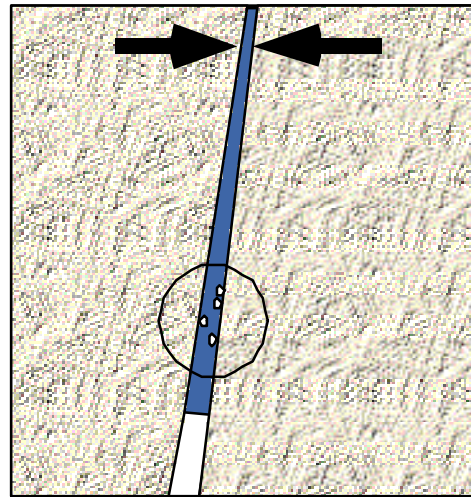
- Bodvarsson, G.S., Boyle, W., Patterson, R. and Williams, D., 1999. Overview of scientific investigations at Yucca Mountain-the potential repository for high-level nuclear waste. *Journal of Contaminant Hydrology*, 38(1-3): 3-24.
- Carter, J.J., 1986. The effects of a clay coating on fluid flow through simulated rock fractures. Masters Thesis, University of California at Berkeley, Berkeley, California, 75 pp.
- Faybishenko, B.A., 1995, Hydraulic behavior of quasi-saturated soils in the presence of entrapped air: Laboratory experiments. *Water Resources Research*, 31(10): 2421-2435.
- Moyer, T.C., Geslin, J.K. and Flint, L.E., 1996. Stratigraphic Relations and Hydrologic Properties of the Paintbrush Tuff Nonwelded (PTn) Hydrologic Unit, Yucca Mountain, Nevada. Open-File Report 95-397, U.S. Geological Survey, Denver, CO.
- Norrish, K., 1955. The swelling of montmorillonite, *Discussions of the Faraday Society*, 18: 120-134.
- Salve, R., and C. M. Oldenburg, Water flow in a fault in altered nonwelded tuff. (*Water Resour. Res.*). (in press)
- Scheidegger, A.E., 1974. *The Physics of Flow through Porous Media*. The University of Toronto Press, 353 pp., p 102.



a.



b.



c.

Figure 1. Possible flow reducing mechanisms. a. Lower-head gradient at later times, b. Imbibition, c. Aperture narrowing due to swelling (arrows) and particle redistribution (circle). Dark color represents liquid water, white represents air.

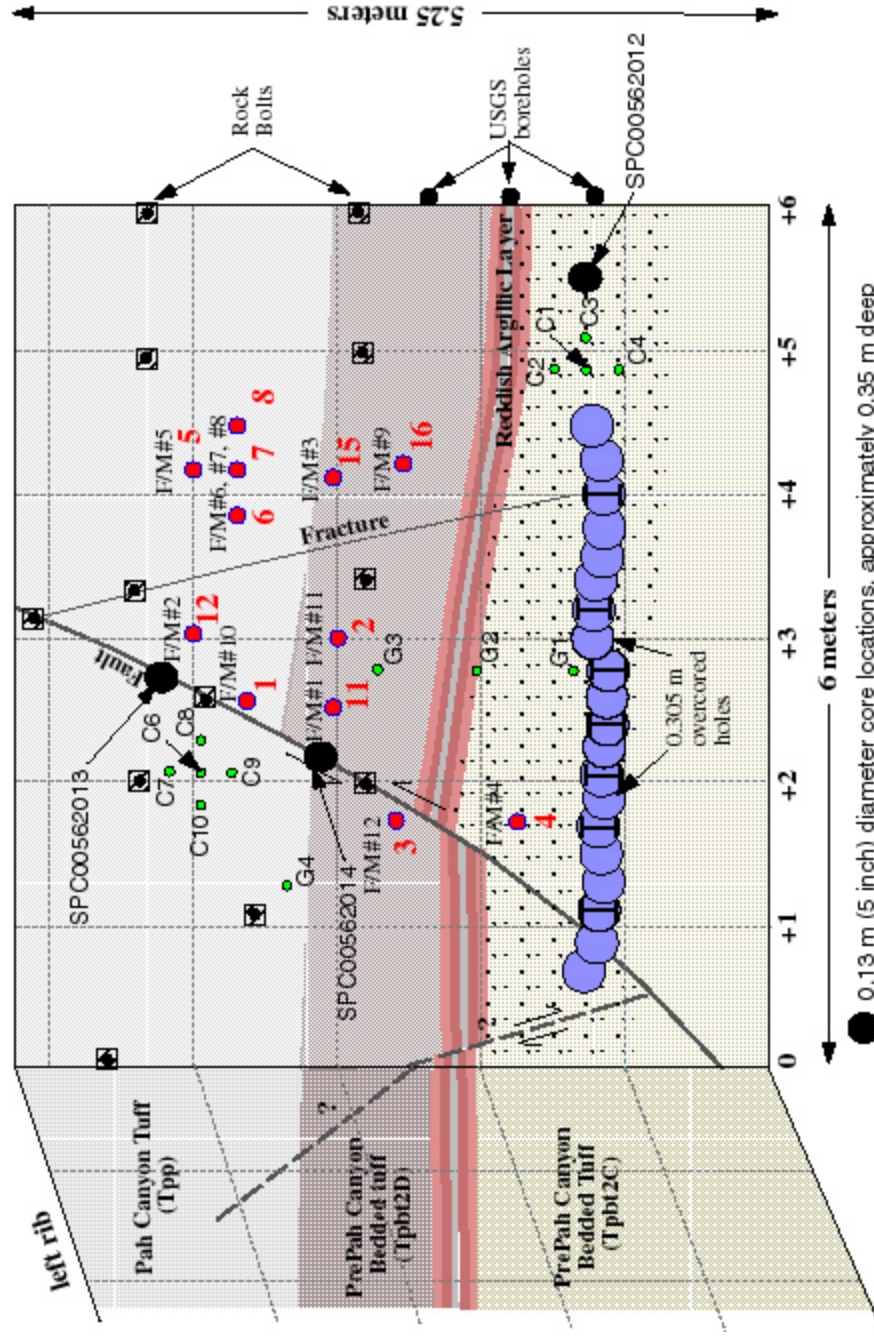


Figure 2. Geological sketch of the north face of Alcove 4 showing core locations, boreholes, and slot.





Figure 3. PTn rock core sample SPC 00562012.

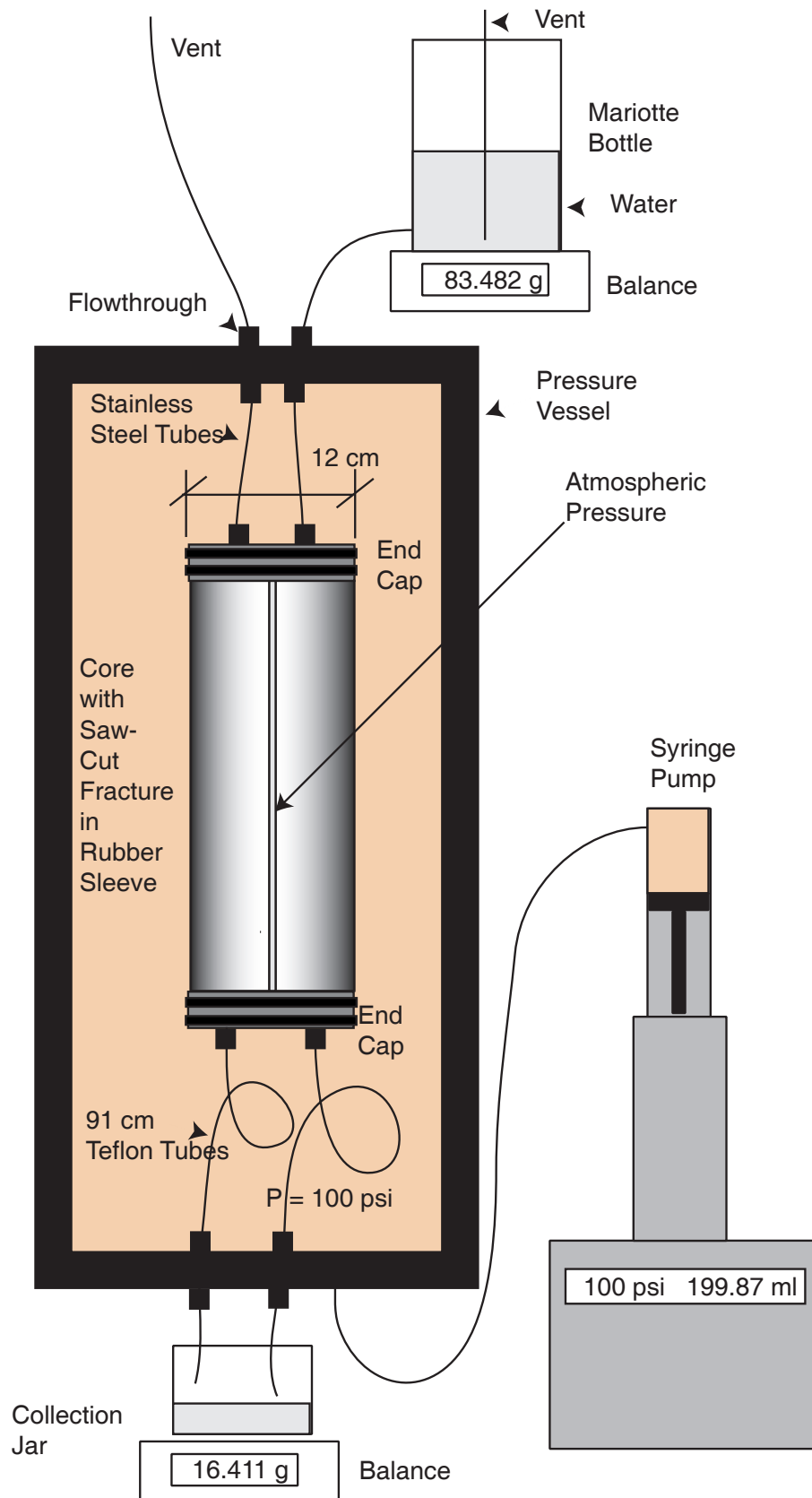


Figure 4. Experiment schematic.

Note: Not to scale

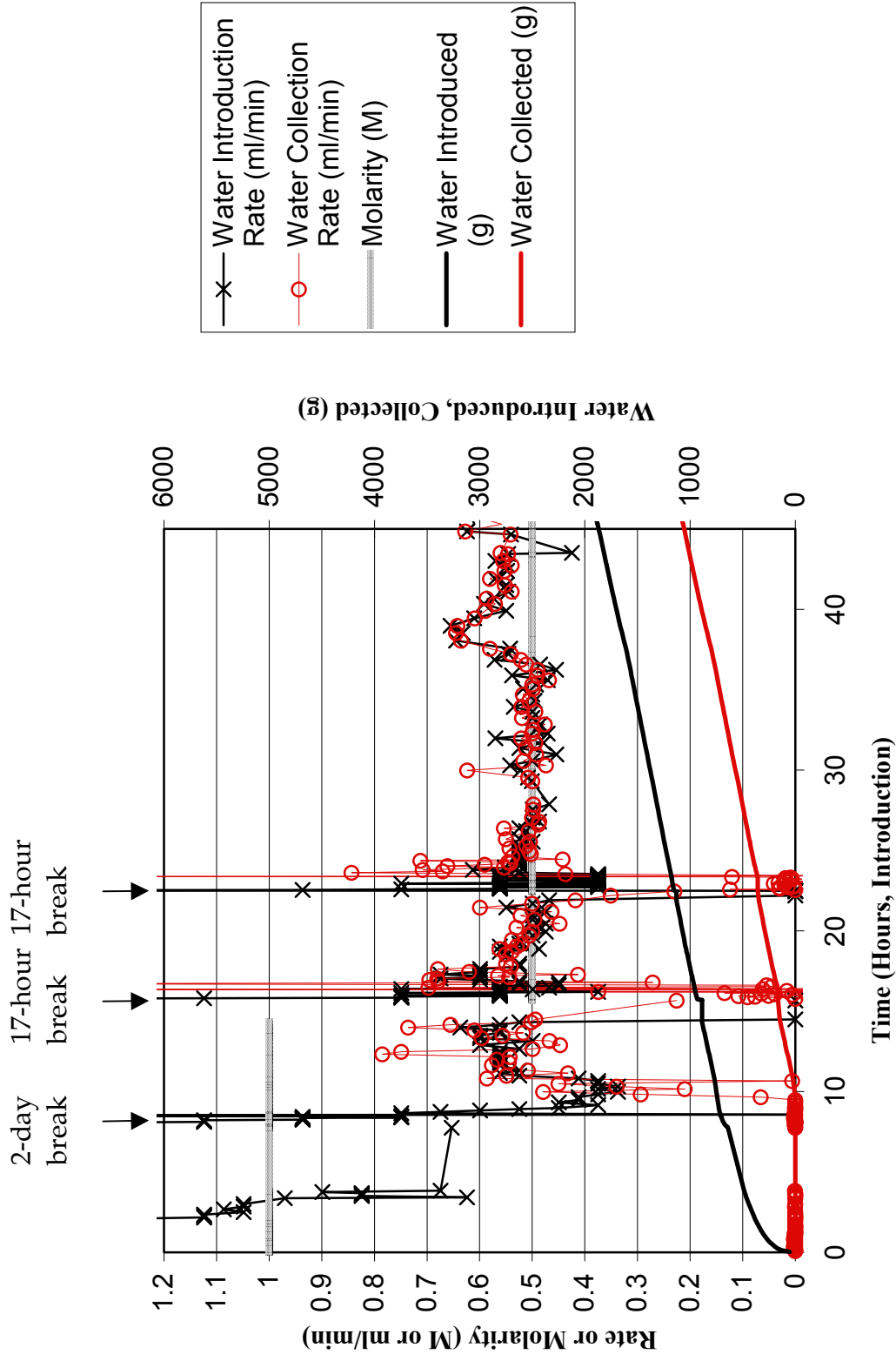


Figure 5a. Volumes and rates of water introduced and collected.

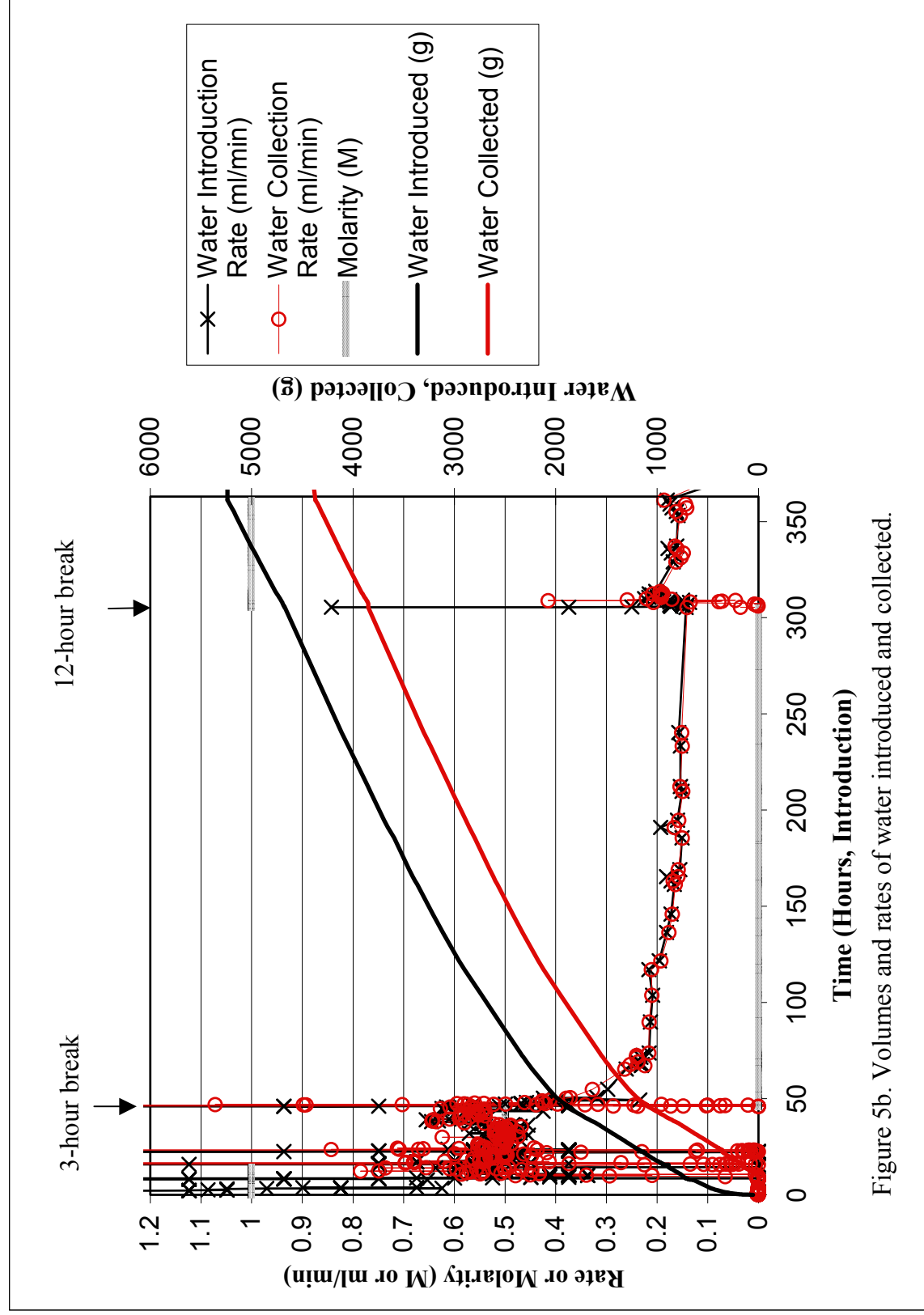


Figure 5b. Volumes and rates of water introduced and collected.

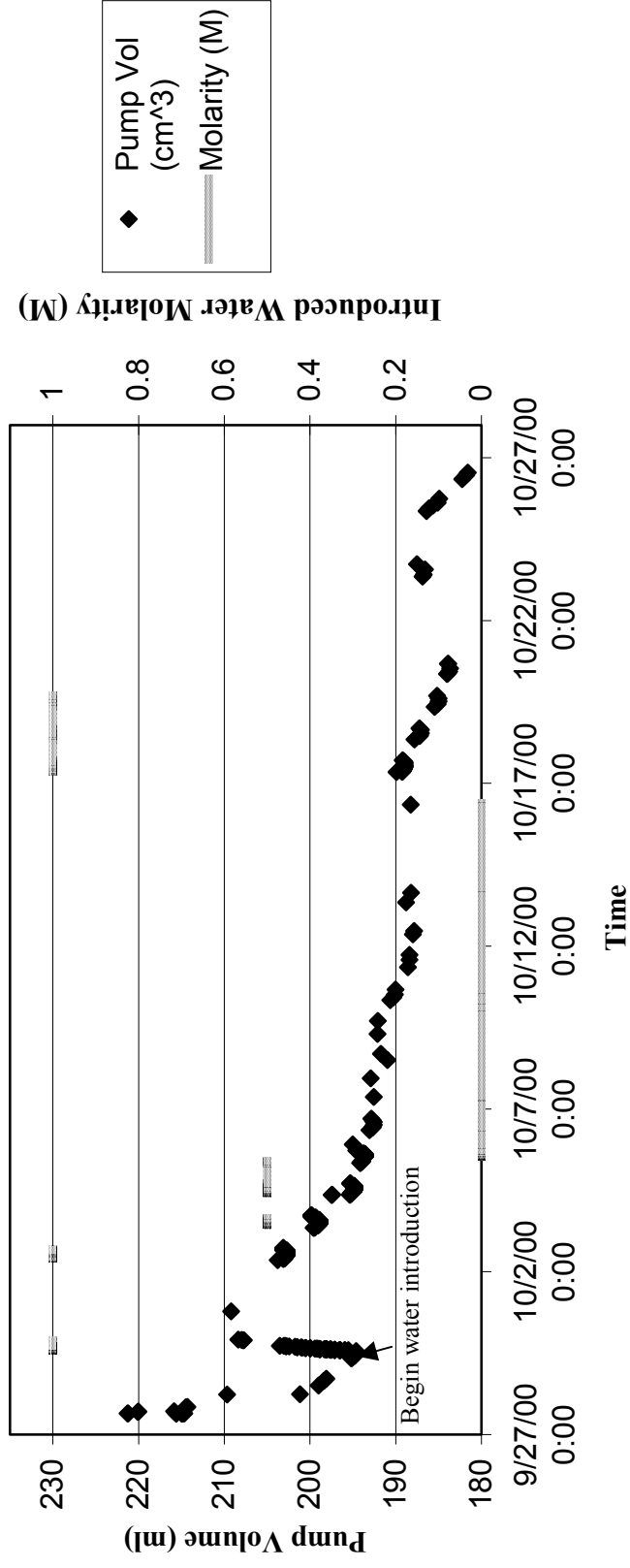


Figure 6a. Syringe pump volume. Increases indicate swelling, decreases indicate shrinkage and leakage.



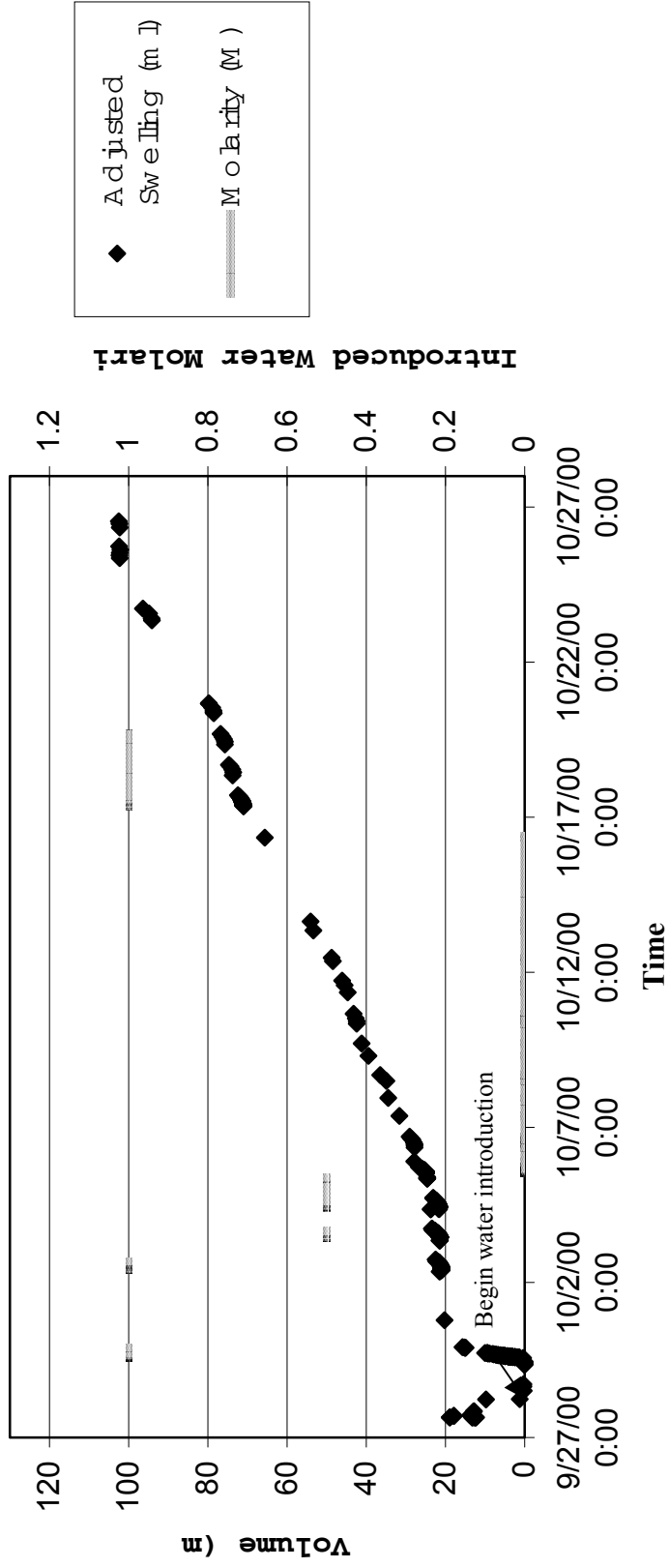


Figure 6b. Adjusted sample swelling. Increases indicate swelling, decreases indicate shrinking or leakage.

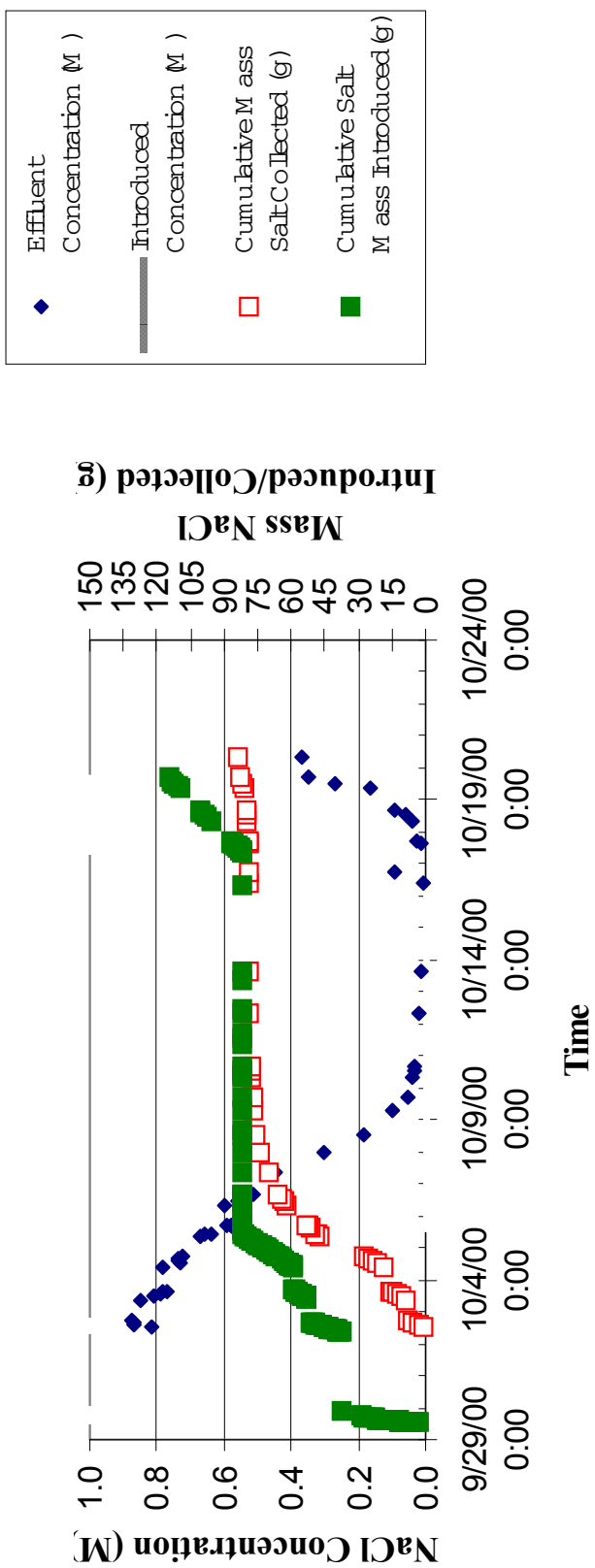


Figure 7. Influent/effluent NaCl concentration (M) and mass balance.



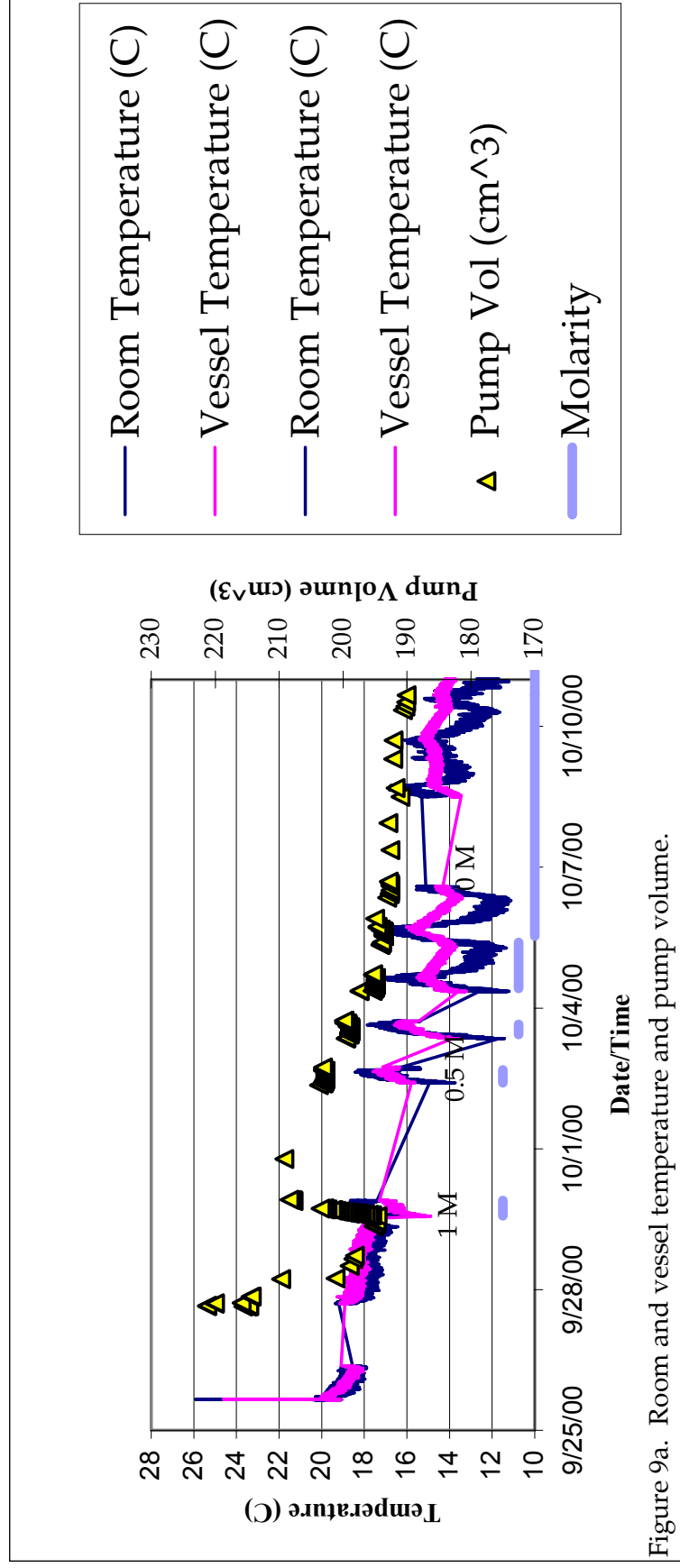


Figure 9a. Room and vessel temperature and pump volume.

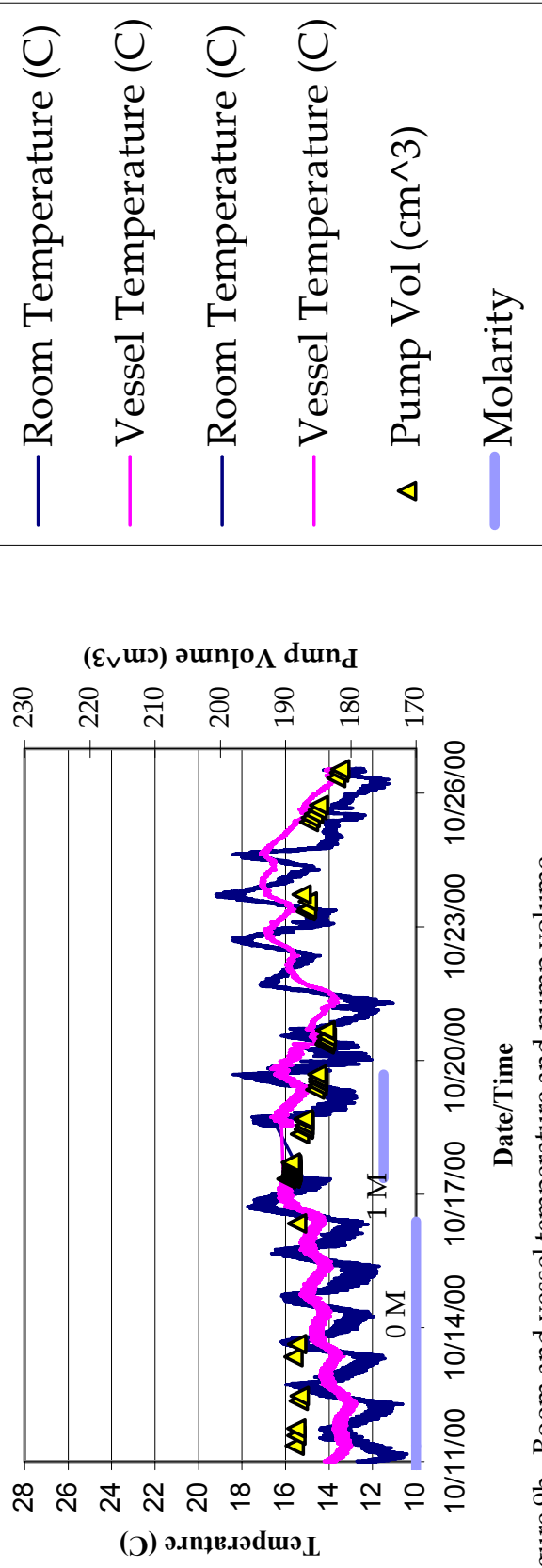


Figure 9b. Room and vessel temperature and pump volume.